MEMS Test Bench and its Uncertainty Analysis for Evaluation of MEMS Mirrors ⋆

Han Woong Yoo * **David Brunner** * **Thomas Thurner** ** **Georg Schitter** *

* *Automation and Control Institute (ACIN), TU Wien, Gusshausstr. 27-29, 1040 Vienna, Austria (e-mail: {yoo, brunner, schitter}@acin.tuwien.ac.at).*
** *Design Center Graz, Infineon Technologies Austria AG, Babenbergerstr. 10, 8020 Graz, Austria (e-mail: Thomas.Thurner@infineon.com)*

Abstract: This paper proposes a MEMS test bench to ensure highly accurate and precise angle measurements for evaluation of multiple MEMS mirrors and analyzes its measurement uncertainty. The MEMS test bench includes a position sensitive detector (PSD) with a motorized stage to convert the beam displacement on the PSD to a mirror angle measurement by a dedicated calibration procedure. Uncertainties in the angle measurement of the MEMS mirrors are analyzed considering the optical alignment, the characterization of the PSD, and the calibration data. By the proposed uncertainty analysis, the accuracy of the developed MEMS test bench shows up to 0.026° at the mirror angle of 15°.

Keywords: Metrology, Uncertainty analysis, Characterization, Microelectromechanical systems (MEMS), MEMS mirror

1. INTRODUCTION

Micro-electro-mechanical systems (MEMS) based scanning mirrors are miniaturized mechatronic systems that consist of an optical micromirror and its actuation scheme to steer the laser beam. With abundant applications, MEMS mirrors receive much attention from pico projector (Yalcinkaya et al. (2006)) to the automotive lidar (Ito et al. (2013); Druml et al. (2018)) thanks to their compactness, robustness, scalability, easy means for integration, and cost-effectiveness (Patterson et al. (2004)). Especially for the automotive lidar application, high accuracy and precision scanning of MEMS mirror is critical to ensure safety of drivers and passengers in various driving conditions such as highways and urban areas (Yoo et al. (2018)).

To ensure the performance of the MEMS mirror, accurate and precise characterization is crucial not only for inspection in production line but also for design of the MEMS mirror to identify the critical parameters to be improved (Brunner et al. (2019)). The characterization setup should provide the measurements in a standard unit, e.g. mirror angle in degree, for comparative analysis of a number of tests of multiple mirrors. For MEMS mirror characterization, the simplest method is an optical leverage with a flat screen with a long distance (Koh and Lee (2012); Kim et al. (2017)). The main advantage is high accuracy by taking a long distance between the mirror and the screen. However, the dynamic behavior of the MEMS mirror is difficult to be recorded, which is critical for the characterization of resonant MEMS mirrors with a few kHz resonance frequency. To measure the dynamics of the MEMS mirror, a laser Doppler vibrometer (LDV) is applied (Rembe et al. (2001); Yalcinkaya et al. (2006); Isikman et al. (2007); Koh and Lee (2012)). LDV provides precise position displacement of the MEMS mirror in real time, but it is expensive and bulky for inspection purpose of multiple MEMS mirrors. With the optical leverage, a position sensitive detector (PSD), which is a special type of photodiode for measuring displacement of the beam center, can be used for the dynamic behavior of the MEMS mirror (Isikman et al. (2007); Kim et al. (2017)). For large mechanical mirror angle measurements over ±10°, PSDs have difficulties to keep the accuracy in the angle measurement due to the limited size of the PSD. The small size of the PSD with a large mirror angle allows only a short distance between the mirror and the PSD, which requires high accuracy of the distance measurements due to high error sensitivity. Innate distortion of PSDs can reduce the accuracy of the mirror angle measurement as well. Therefore, PSD measurements are usually provided as an additional information with other measurement such as a screen (Kim et al. (2017)) or a LDV (Isikman et al. (2007)).

This paper proposes a PSD based MEMS test bench for characterization of multiple 1D resonant MEMS scanning mirrors and analyzes potential uncertainties of the mirror angle measurement. The designed MEMS test bench provides a calibration procedure with a motorized stage, enabling accurate and precise mirror angle measurements. To evaluate the uncertainty of the angle measurements, measurement errors by the PSD, the optical alignment,

⋆ This work has been supported in part by the Austrian Research Promotion Agency (FFG) under the scope of the LiDcAR project (FFG project number 860819).

Post-print version of the article: H. W. Yoo, D. Brunner, T. Thurner, G. Schitter, "MEMS Test Bench and its Uncertainty Analysis for Evaluation of MEMS Mirrors," *8th IFAC Symposium on Mechatronic Systems*, vol. 52, no. 15, pp 49-54, 2019. DOI: 10.1016/j.ifacol.2019.11.648

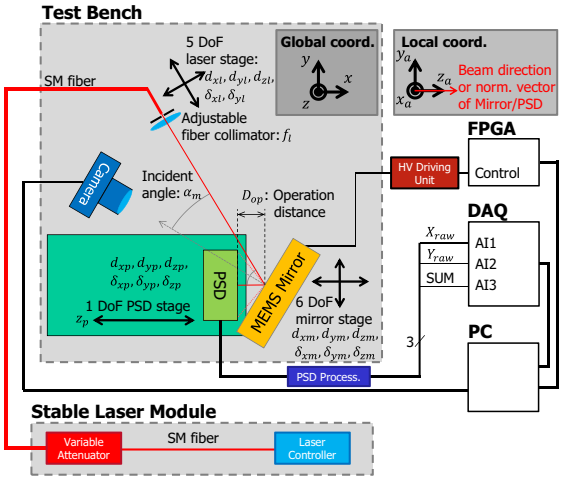

(a) Schematics

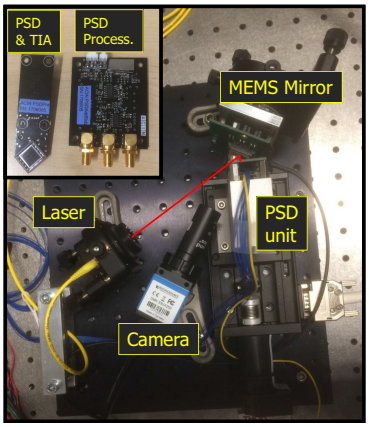

(b) Picture of test bench

Fig. 1. Schematic diagram (top) and a picture (bottom) of the MEMS test bench. For the accurate alignment and calibration, the laser, the mirror, and the PSD are mounted on a 5 DoF optics mount, a 6 DoF mirror mount, and a 1 DoF motorized stage, respectively.

and the calibration procedure are analyzed with their sensitivity functions. With measurement data from the calibration procedure, the angle measurements uncertainty is calculated to verify the characterization performance of the designed MEMS test bench.

2. DESIGN AND MODELING

2.1 Design of MEMS Test Bench

Fig. 1 illustrates a schematic diagram and a picture of the MEMS test bench. A single mode fiber laser source (S1FC635, 635 nm, 2.5 mW, Thorlabs, Newton, NJ, USA) is connected to a variable fiber attenuator (VOA630-FC, 630 nm, $<$ 50 dB, Thorlabs) to secure class 1 operation. The attenuated laser shines on the MEMS mirror and focused by an adjustable fiber collimator (CFC-5X-A, Thorlabs) on the PSD (S5991-01, 2D PSD, 9×9 mm, Hamamatsu, Hamamatsu City, Japan), which provides high linearity in a wide range with relatively small nonlinear distortion. For precision alignment, the laser collimator and the mirror are mounted on a 5 degree of freedom (DoF) mount (K5X1, Thorlabs) and a 6 DoF mount (K6XS, Thorlabs), enabling the correction in all possible axes of position and rotations. For correction of the error after replacement of the mirror, the mirror position and the beam position at the mirror is measured by a CMOS camera (DMK 33UX252, The Imaging Source, Bremen, Germany) with an objective (Telecentric Lens, ×1, f = 40 mm, Edmund optics).

The photo current from PSD is processed by separated two modules, which are trans-impedance amplifiers (TIA) module and position process module. The TIA module changes the weak photo current to voltage and the position process module changes the voltage of the PSD electrodes to the position X_{raw}, Y_{raw} and intensity SUM information. In the TIA module, the PSD is mounted with an angle of 45° to use a long diagonal axis for the scan trajectory measurement and TIAs are installed on the backside of PSD. To reduce electromagnetic interference (EMI) by the high voltage operation of the MEMS mirror, a pair of metal shield covers the PSD and TIAs. The TIA module with PSD is attached on a CNC-machined steel mount and installed on a 1D motorized stage (VT-80 62309110, 25 mm range, 0.5 μm resolution, Physik Instrumente, Karlsruhe, Germany), which provides room for the mirror exchange and enable a calibration procedure to convert the PSD measurement to the mirror angle measurement.

The computer controls the motorized stage and records the PSD data by a DAQ module (U2531A, 2 MSps, Keysight, Santa Rosa, CA, USA). The mirror is operated by a standalone FPGA board (Zedboard, Avnet, Phoenix, AZ, USA). The mirror control signal is applied to a custom-made high voltage driver circuit to drive the MEMS mirror with a high voltage up to 150 V (Brunner et al. (2019)).

2.2 Ray Tracing Model of MEMS Test bench

Fig. 1a also contains the global coordinate system for the beam propagation description from the laser to the PSD. The rotation axis of the MEMS mirror is set at the origin of the global coordinate system. The mirror surface at the zero mirror angle is defined by a normal vector $\boldsymbol{n}_{m0}$ and a position vector $\boldsymbol{p}_{m0}$. The surface plane of the scanning mirror with a mechanical mirror angle θ_m can be describe as

$$0 = \boldsymbol{n}_m^T(\theta_m)\left(\boldsymbol{r} - \boldsymbol{p}_m(\theta_m)\right), \quad (1)$$

$$\boldsymbol{n}_m(\theta_m) = R(\theta_m, \boldsymbol{r}_m)\boldsymbol{n}_{m0}, \quad (2)$$

$$\boldsymbol{p}_m(\theta_m) = R(\theta_m, \boldsymbol{r}_m)\boldsymbol{p}_{m0}, \quad (3)$$

where $\boldsymbol{a}^T$ denotes transpose of the vector $\boldsymbol{a}$, $\boldsymbol{r}$ denotes position variables, i.e. $\boldsymbol{r} = [\,x\ y\ z\,]^T$. $\boldsymbol{n}_m(\theta_m)$ and $\boldsymbol{p}_m(\theta_m)$ denote the normal vector and the position vector of the mirror surface with a mechanical mirror angle θ_m, respectively. $R(\theta_m, \boldsymbol{r}_m)$ is a 3D rotation matrix with a mechanical mirror angle θ_m along the rotation axis of the mirror $\boldsymbol{r}_m = [\,r_{m,x}\ r_{m,y}\ r_{m,z}\,]^T$. From the laser position vector $\boldsymbol{p}_l$ and the laser direction vector $\boldsymbol{u}_l$, the position of the

Post-print version of the article: H. W. Yoo, D. Brunner, T. Thurner, G. Schitter, "MEMS Test Bench and its Uncertainty Analysis for Evaluation of MEMS Mirrors," *8th IFAC Symposium on Mechatronic Systems*, vol. 52, no. 15, pp 49-54, 2019.
DOI: 10.1016/j.ifacol.2019.11.648

mirror reflection $\boldsymbol{p}_{lm}$ and the direction of reflection $\boldsymbol{u}_{lm}$ is obtained by

$$\boldsymbol{p}_{lm}(\theta_m) = \boldsymbol{p}_l + \frac{\boldsymbol{n}_m^T(\theta_m)(\boldsymbol{p}_m(\theta_m) - \boldsymbol{p}_l)}{\boldsymbol{n}_m^T(\theta_m)\boldsymbol{u}_l}\boldsymbol{u}_l, \quad (4)$$

$$\boldsymbol{u}_{lm}(\theta_m) = \boldsymbol{u}_l - 2\left(\boldsymbol{u}_l^T \boldsymbol{n}_m(\theta_m)\right)\boldsymbol{n}_m(\theta_m). \quad (5)$$

Besides, the surface of the PSD is defined as

$$0 = \boldsymbol{n}_p^T(\boldsymbol{r} - \boldsymbol{p}_p), \quad (6)$$

where $\boldsymbol{p}_p$ and $\boldsymbol{n}_p$ denotes the position and the normal vector of the PSD surface, respectively. The reflected laser beam by the scanning mirror coincides the surface of PSD at

$$\boldsymbol{p}_{mp}(\theta_m) = \boldsymbol{p}_{lm}(\theta_m) + \frac{\boldsymbol{n}_p^T\left(\boldsymbol{p}_p - \boldsymbol{p}_{lm}(\theta_m)\right)}{\boldsymbol{n}_p^T\boldsymbol{u}_{lm}(\theta_m)}\boldsymbol{u}_{lm}(\theta_m). \quad (7)$$

$\boldsymbol{p}_{mp}$ already indicates the position of the beam spot on the PSD surface in the global coordinate system. The beam position output of the PSD can be transformed from the 3D points to a 2D coordinate system by

$$\boldsymbol{p}_{psd}(\theta_m) = kER_{rev}(\boldsymbol{p}_{mp}(\theta_m) - \boldsymbol{p}_p), \quad (8)$$

where R_{rev} is a rotation matrix that change the surface of the PSD to one of 2D coordinate system, and E is a 2×3 matrix to eliminate the unnecessary dimension. k denotes the scaling factor of the PSD, which is discussed further in Sec. 3.1.

2.3 Angle Measurement and Calibration Procedure

Assume that the reflected beam with the zero mirror angle is orthogonal to the projected trajectory on the PSD. Then the mirror angle is obtained by the beam displacement p_θ from the zero angle as

$$\theta_m = \frac{1}{2}\tan^{-1}\left(\frac{p_\theta(\theta_m)}{D_{op}}\right), \quad (9)$$

$$p_\theta(\theta_m) = \boldsymbol{u}_{py}^T\left(\boldsymbol{p}_{psd}(\theta_m) - \boldsymbol{p}_{psd}(0)\right), \quad (10)$$

where D_{op} denotes an operation distance from the mirror surface to the PSD and $\boldsymbol{u}_{py}$ is the unit vector of y direction of the PSD which is parallel to the ideal beam trajectory on the PSD. The beam displacement is defined by a projection on the scanning axis on the PSD, i.e. the inner product of the beam displacement and the beam scan direction. An accurate measurement of the operation distance is difficult because the space between PSD to the mirror is only a few mm excluding the packages of the mirror and the shield of the PSD.

Calibration of the MEMS test bench is a procedure to estimate the operation distance D_{op} by multiple measurements of a scan trajectory. Fig. 2 describes the basic idea of calibration procedure by moving the PSD unit while the MEMS mirror is running at a fixed amplitude. Assume that the mechanical scan trajectory is a periodic function with an amplitude Θ_m and a zero offset. An estimated operation distance can be obtained by

$$D_{op} = a(\Theta_m)\, p_{pp}(d_{zp}, \Theta_m) - d_{zp}, \quad (11)$$

$$p_{pp} = \boldsymbol{u}_{py}^T\left(\boldsymbol{p}_{psd}(\Theta_m) - \boldsymbol{p}_{psd}(-\Theta_m)\right), \quad (12)$$

where p_{pp} denotes the peak to peak displacement of the scan trajectory, and d_{zp} denotes the displacement of the PSD by the motorized stage. $a(\Theta_m)$ is the slope $a(\Theta_m)$, defined as $a(\Theta_m) = \frac{1}{2\tan(2\Theta_m)}$. The estimation of operation distance $\hat{D}_{op}$ is obtained by solving a linear regression of

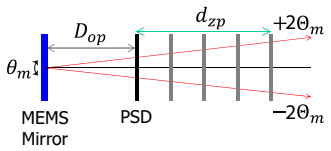

Fig. 2. Calibration process of the MEMS test bench with a fixed amplitude Θ_m. The operation distance D_{op} is estimated by the projected peak to peak displacement p_{pp} on the PSD while the stage moves the PSD at multiple distances with d_{zp}.

(11) with multiple measurements of p_{pp} with various d_{zp}. The estimation of the slope $\hat{a}$ is automatically obtained by the linear regression as well. Then the measured mechanical mirror angle with the calibration can be written as

$$\hat{\theta}_m = \frac{1}{2}\tan^{-1}\left(\frac{p_\theta(\theta_m)}{\hat{D}_{op}}\right). \quad (13)$$

3. UNCERTAINTY ANALYSIS

In this section, potential error sources and their uncertainties are analyzed for the evaluation of the mirror angle measurement. The errors in the PSD measurement, misalignment of the optical setup, and the calibration error can be considered as dominant error sources in the MEMS test bench. By assuming that all error sources are independent, the standard deviation of the beam displacement error can be written as

$$\sigma_{p_\theta}^2 = \sigma_{psd}^2 + \sigma_{opt}^2, \quad (14)$$

where σ_{psd} and σ_{opt} denote the standard deviation caused by PSD and optical alignment, respectively. The errors of the calibration and the mirror angle measurement are analyzed based on the errors of the beam displacement. The details of each error source are discussed in the following subsections.

3.1 Uncertainty in PSD measurement

Since the PSD is the main sensor of the MEMS test bench, errors in the PSD measurement are important to be analyzed. Three error sources can be considered in the PSD measurements, which are a scale error, an accuracy error, and a precision error. First, the scale error of the PSD is the errors in scaling of the PSD position calculation, described by k_Δ from $k = k_0(1 + k_\Delta)$, where k_0 denotes the nominal scaling factor. This scale error can be caused by the inaccurate the calibration of the PSD, temperature variation, and gain mismatch in analog unit (Yoo et al. (2019)). Secondly, the accuracy error is the error due to the distortion of the PSD measurements, which can be defined as a residual position error or nonlinear distortion after the correction of the scaling error. Last, the precision error is an uncertainty of the PSD measurement by the noise of the signal. The precision error changes by the bandwidth and can be improved by averaging in offline analysis such as the calibration procedure.

Fig. 3 illustrates the measured accuracy error and precision errors of a PSD along the two diagonal axes by the PSD

Post-print version of the article: H. W. Yoo, D. Brunner, T. Thurner, G. Schitter, "MEMS Test Bench and its Uncertainty Analysis for Evaluation of MEMS Mirrors," *8th IFAC Symposium on Mechatronic Systems*, vol. 52, no. 15, pp 49-54, 2019. DOI: 10.1016/j.ifacol.2019.11.648

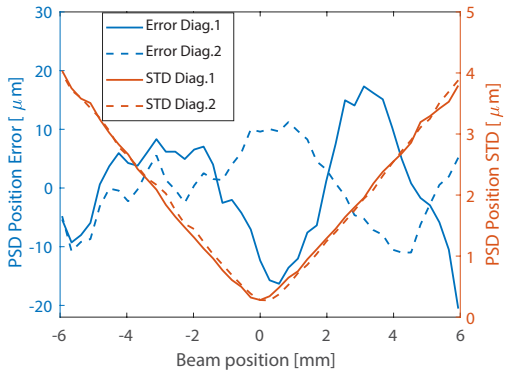

Fig. 3. Measured accuracy error and precision of the PSD along two diagonal axes.

characterization setup in (Yoo et al. (2019)). The errors in diagonal axis shows the measurement accuracy of the PSD, whose standard deviations $\sigma_{psd,acc}$ are $9.39\mu m$ and $6.37\mu m$ for each diagonal axis 1 and 2, respectively. For the correction of the line error, the PSD scale error k_Δ of the diagonal axis 1 and 2 are obtained as 0.89×10^{-3} and -0.65×10^{-3} for $k_0 = 0.994$, respectively. The standard deviation is measured with 20 kHz band-limited signals (Brunner et al. (2019)), showing a linear behavior along the absolute beam displacement with a range from 0.28 μm to $4.04\mu m$. Assuming $p_{psd}(0)$ is at the center of PSD, the model of the PSD noise can be written as

$$\sigma_{psd}^2 = \sigma_{psd,acc}^2 + p_\theta^2(\theta_m)\sigma_{psd,k_\Delta}^2 + \sigma_{psd,pre}^2(p_\theta(\theta_m)), \quad (15)$$

$$\sigma_{psd,pre}(p_\theta(\theta_m)) = \frac{1}{\sqrt{N}}(\sigma_{psd,pre0} + \sigma_{psd,pre1}|p_\theta(\theta_m)|), \quad (16)$$

where $\sigma_{psd,pre0}$ and $\sigma_{psd,pre1}$ are fitting parameters to the measurement of standard deviation of precision error and N is the number of average. For further analysis, $\sigma_{psd,k_\Delta} = 0.001$ with $k_0 = 0.994$, considering the measured scale factors of along the diagonal axes. For the precision error, $\sigma_{psd,pre1} = 6.402 \times 10^{-4}$, and $\sigma_{psd,pre0} = 7.15 \times 10^{-5}$ mm. Besides, for the case of the PSD accuracy $\sigma_{psd,acc}$, the actual accuracy of the PSD in the MEMS test bench can be reduced due to filtering along the the scanning trajectories and it can be estimated during the calibration procedure. Further discussion follows in Sec. 3.3.

3.2 Uncertainty in Optical Alignment

The alignment for laser, mirror and PSD can be described by the local coordinate systems in Fig. 1a. For example of the laser, z_l axis is aligned by the beam direction, x_l axis is orthogonal to the breadboard, and y_l axis is orthogonal to z_l and x_l, which is parallel to the breadboard surface. For the mirror and the PSD, the normal vector of the surface plane is aligned with z_m and z_p axis, respectively, and other axes are defined in the same manner. For the defined axis, for example of x_l, the translation positions errors and the rotational errors are defined as d_{xl} and δ_{xl}, respectively.

The ideal alignment can be defined by four conditions. First, the height of laser beam, mirror, and the diagonal axis of the PSD are at the same height and beam does not change the height, which leads to $d_{xl} = d_{xm} = d_{xp}$ and $\delta_{yl} = \delta_{ym} = 0$. Second, the laser beam from the MEMS mirror is perpendicular to the y axis of the PSD, i.e. $\delta_{xp} = 0$ and $\delta_{xm} = 0$, and is parallel to the moving axis of the motorized stage. Third, the laser beam shines at the center of the mirror where the rotational axis is located, i.e. $d_{yl} = 0$. Lastly, the operation distance is less than 10.4 mm to cover the mirror angle of 15° with a reasonable accuracy of the PSD.

The alignment procedure is to fix each source of errors in the local coordinate systems of the laser beam, MEMS mirror, and the PSD. For the height alignment, the laser and the PSD are aligned with a long distance over 20 cm, and the height and angle error of the laser are adjusted. Tip tilt errors of the mirror, δ_{xm} and δ_{ym}, are roughly aligned with the laser, and are finely aligned by minimizing the variation of the beam displacement along the movement of the motorized stage. The alignment of the PSD tilt angle δ_{xp} is defined by the CNC-machined solid mount, and the beam center on the mirror surface can be aligned by the images of the MEMS mirror and the beam spot by the camera. The operation distance is discussed further in the following subsection about the calibration procedure.

After the alignment procedure, residual uncertainties in the optical alignment influence the uncertainty of the beam displacement. Four main sources of the optical alignment error can be considered, which are the mirror tilt error δ_{xm}, the mirror tip error δ_{ym}, the PSD tilt error δ_{xp}, and the laser lateral misalignment d_{yl}. The laser lateral misalignment d_{yl} defines the misalignment of the laser beam to the mirror rotation center with the incident angle α_m. By applying the global coordinate system, the position and direction vectors of the laser, the MEMS mirror, and the PSD are defined as follows.

$$\begin{aligned}
\boldsymbol{p}_l &= \begin{bmatrix} d_{lm}\cos(\pi - 2\alpha_m) + d_{yl}\cos(\pi/2 - 2\alpha_m) \\ d_{lm}sin(\pi - 2\alpha_m) + d_{yl}\sin(\pi/2 - 2\alpha_m) \\ 0 \end{bmatrix}, \\
\boldsymbol{u}_l &= -\begin{bmatrix} d_{lm}cos(\pi - 2\alpha_m) \\ d_{lm}sin(\pi - 2\alpha_m) \\ 0 \end{bmatrix}, \\
\boldsymbol{p}_p &= \begin{bmatrix} -D_{op} \\ 0 \\ 0 \end{bmatrix}, \quad \boldsymbol{n}_p = \begin{bmatrix} \sin(\pi/2 - \delta_{yp})\cos\delta_{xp} \\ \sin(\pi/2 - \delta_{yp})\sin\delta_{xp} \\ \cos(\pi/2 - \delta_{yp}) \end{bmatrix}, \\
\boldsymbol{p}_{m0} &= \begin{bmatrix} 0 \\ 0 \\ 0 \end{bmatrix}, \ \boldsymbol{n}_{m0} = \begin{bmatrix} \sin(\pi/2 - \delta_{ym})\cos(\pi - (\alpha_m + \delta_{xm})) \\ \sin(\pi/2 - \delta_{ym})\sin(\pi - (\alpha_m + \delta_{xm})) \\ \cos(\pi/2 - \delta_{ym}) \end{bmatrix}, \\
\boldsymbol{r}_m &= \begin{bmatrix} \sin\delta_{ym}\sin(\pi - \alpha_m) \\ \sin\delta_{ym}\cos(\pi - \alpha_m) \\ \cos\delta_{ym} \end{bmatrix}. \quad (17)
\end{aligned}$$

where d_{lm} denotes the distance from the laser to the mirror, which is set to 24 mm. δ_{yp} denotes the tip angle of the PSD, i.e. 7°. For the simulation, the incident angle α_m is set to 20°. The operation distance D_{op} is set to 9.618 mm to match the value with the calibration result (c.f. Sec. 4). The uncertainties of the optics misalignment can be written as

Post-print version of the article: H. W. Yoo, D. Brunner, T. Thurner, G. Schitter, "MEMS Test Bench and its Uncertainty Analysis for Evaluation of MEMS Mirrors," *8th IFAC Symposium on Mechatronic Systems*, vol. 52, no. 15, pp 49-54, 2019.
DOI: 10.1016/j.ifacol.2019.11.648

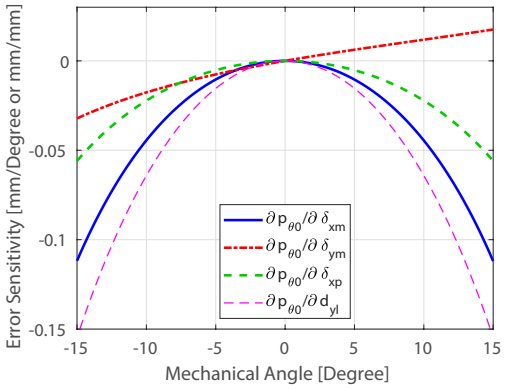

Fig. 4. Sensitivity functions of the uncertainties by optical alignment.

$$\sigma_{opt}^2 = \left(\frac{\partial p_\theta(\theta_m)}{\partial \delta_{xm}}\right)^2 \sigma_{\delta_{xm}}^2 + \left(\frac{\partial p_\theta(\theta_m)}{\partial \delta_{ym}}\right)^2 \sigma_{\delta_{ym}}^2 + \left(\frac{\partial p_\theta(\theta_m)}{\partial \delta_{xp}}\right)^2 \sigma_{\delta_{xp}}^2 + \left(\frac{\partial p_\theta(\theta_m)}{\partial d_{yl}}\right)^2 \sigma_{d_{yl}}^2, \quad (18)$$

where $\sigma_{\delta_{xm}}$, $\sigma_{\delta_{ym}}$, $\sigma_{\delta_{xp}}$, and $\sigma_{d_{xl}}$ are corresponding standard deviation of δ_{xm}, δ_{ym}, δ_{xp}, and d_{yl}, respectively. The sensitivity functions of each uncertainty component can be obtained numerically. Fig. 4 shows the sensitivity functions of the uncertainties in the optical misalignment along the mechanical mirror angle. For δ_{xm}, δ_{xp}, and d_{xl}, the sensitivity functions are mainly even functions while δ_{ym} is mixed with an odd function, showing asymmetric sensitivity.

The uncertainties of each component can be obtained by the defined alignment procedure. For example, $\sigma_{\delta_{xm}}$ and $\sigma_{\delta_{ym}}$ can be obtained by accuracy error of PSD between the stage movement of 20 mm, i.e. $\tan^{-1}(\sigma_{psd,acc}/20) \approx 0.027°$. δ_{xp} can be given by the tolerance of the solid block, e.g. 25 μm along two holes with a distance of 34 mm, i.e. $\tan^{-1}(0.025/34) \approx 0.017°$. d_{xl} can be obtained by the quarter of the $1/e^2$ beam diameter at the mirror, i.e. $0.032 \cos\alpha_m \approx 0.030$ mm.

3.3 Uncertainties of Calibration and Estimation of PSD Accuracy Error

The standard deviation of the estimated operation distance $\sigma_{\hat{D}_{op}}$ is obtained by the variance calculation of the residual errors in the linear regression. During the regression, uncertainties in optical alignment and the scaling errors of the PSD do not influence the estimated operation distance since they only change the estimated slope $\hat{a}$. The precision of PSD can be neglected by a large number of averaging as well. Then the uncertainty of the estimated operation distance can be written as

$$\sigma_{\hat{D}_{op}}^2 = \left(\hat{a}(\Theta_m)\right)^2 \sigma_{PSD,acc}^2 + \sigma_{d_{zp}}^2. \quad (19)$$

Since $\sigma_{d_{zp}}^2 > 0$, the accuracy of PSD can be estimated by the calibration procedure as

$$\hat{\sigma}_{psd,acc} = \frac{\sigma_{\hat{D}_{op}}}{|\hat{a}(\Theta_m)|} > \sigma_{psd,acc}. \quad (20)$$

For the uncertainty analysis of the MEMS test bench, this estimated accuracy of PSD is used instead of the measured accuracy of PSD in Sec. 3.1. That is because it is directly measured by the MEMS test bench, and it considers filtering of the scanning trajectory measurements. Therefore the estimated accuracy of PSD is regarded more realistic to be used for the uncertainty analysis.

3.4 Uncertainty in Angle Measurement

From (13), the uncertainty of the measured mechanical angle of the MEMS mirror can be rewritten as

$$\sigma_{\hat{\theta}_m}^2 = \sigma_{\hat{\theta}_{m,psd}}^2 + \sigma_{\hat{\theta}_{m,opt}}^2 + \sigma_{\hat{\theta}_{m,cal}}^2 \quad (21)$$

$$= \frac{\sigma_{psd}^2}{4\hat{D}_{op}^2\left(1+\frac{p_\theta^2}{\hat{D}_{op}^2}\right)^2} + \frac{\sigma_{opt}^2}{4\hat{D}_{op}^2\left(1+\frac{p_\theta^2}{\hat{D}_{op}^2}\right)^2} + \left(\frac{-p_\theta}{2\hat{D}_{op}^2\left(1+\frac{p_\theta^2}{\hat{D}_{op}^2}\right)}\right)^2 \sigma_{\hat{D}_{op}}^2, \quad (22)$$

where $\sigma_{\hat{\theta}_{m,psd}}$, $\sigma_{\hat{\theta}_{m,opt}}$, and $\sigma_{\hat{\theta}_{m,cal}}$ denote the uncertainty of the angle measurements contributed by the the PSD, the optical alignment, and the calibration. The other error sources except for parameters from calibration are already available based on the prior measurements and assumptions. This uncertainty of the mirror angle measurement can be calculated by the calibration process of the measurements, discussed in the following section.

4. CALIBRATION AND UNCERTAINTY EVALUATION

This section describes the measurement results of the proposed calibration procedure and derives the uncertainty of the MEMS test bench based on the estimated parameters from the calibration. First, the calibration measurements is analyzed to estimate the operation distance, the variance of operation distance, and the accuracy error of PSD. For the experiment, a MEMS mirror in (Brunner et al. (2019)) is used for the evaluation of the MEMS test bench and the calibration procedure. While the mirror is running with an unknown amplitude, the beam trajectory measurements by the PSD are recorded for 23 measurement points from 0 to 22 mm. The peak to peak displacement for each point is obtained by averaging 42 periods of the mirror scanning trajectories.

Fig. 5 illustrates measured peak to peak displacements, the estimated affine function, and the residual PSD errors from the estimation. The zero crossing (red circle) of the estimated affine function indicates the estimated operation distance of the mirror, which $\hat{D}_{op} = 9.618$ mm. The standard deviation of the estimated operation distance is obtained by the covariance of the estimation, i.e. $\sigma_{\hat{D}_{op}} = 6.55$ μm. The estimated accuracy of the PSD $\hat{\sigma}_{psd,acc}$ is 2.01 μm since the estimated slope $\hat{a}$ is 3.26.

Fig. 6 shows the angle measurement uncertainty along mechanical mirror angle and the contribution of each uncertain components in PSD and optical alignment. The left figure illustrates the uncertainty of the mirror angle

Post-print version of the article: H. W. Yoo, D. Brunner, T. Thurner, G. Schitter, "MEMS Test Bench and its Uncertainty Analysis for Evaluation of MEMS Mirrors," *8th IFAC Symposium on Mechatronic Systems*, vol. 52, no. 15, pp 49-54, 2019. DOI: 10.1016/j.ifacol.2019.11.648

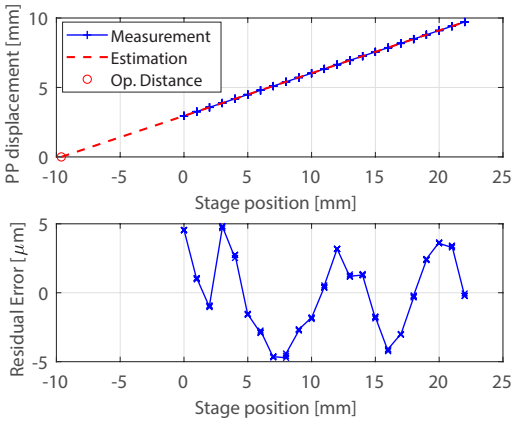

Fig. 5. (Top) Calibration result with the motorized stage for every mm from 0 to 22 mm. (Bottom) residual error after the linear regression.

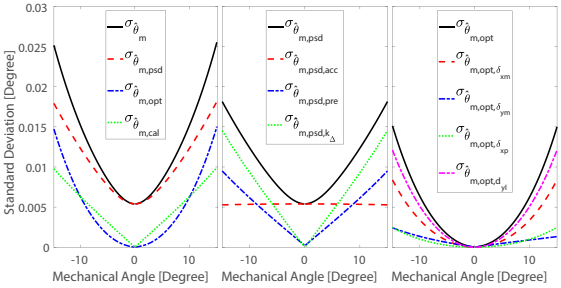

Fig. 6. Uncertainties in the angle measurements along the mechanical mirror angle and its component-wise contribution by PSD and optical alignment.

measurement and the contribution of the PSD, optical alignment, and the calibration. The middle and the right figures show the error components in the mirror angle measurement uncertainty by PSD and optical alignment, respectively. The uncertainty of the angle measurements increases from 0.005° to 0.026° as the absolute mechanical angle increases. The main contribution at a large mirror angle over 10° is given by scaling error in PSD, followed by optical alinement error of d_{yl} and the uncertainty of the calibration.

This result shows that designed MEMS test bench can achieve 0.026° anglular uncertainties by design, and the proposed uncertainty analysis can provide information about main error sources to be considered in the mirror angle measurements.

5. CONCLUSION

This paper proposes a MEMS test bench based on a PSD and analyzes its uncertainty to ensure highly accurate and precise mirror angle measurement for a 1D resonant MEMS mirror. The MEMS test bench is equipped for a PSD module mounted on a motorized stage, enabling a precision conversion from the beam displacement to the mechanical mirror angle of the MEMS mirror. In the MEMS test bench, the laser and the MEMS mirror are mounted by a 5 DoF and a 6 DoF manual mount, respectively, to compensate for all potential misalignment in the optical path. For the uncertainty analysis, the optical path of the MEMS test bench is modeled as vector equations to derive sensitivity functions of the angle measurements for the uncertainties of the PSD, the alignment of the optical setup, and the calibration procedure. The analysis based on the measured calibration procedure reveals that the developed MEMS test bench shows up to 0.026° of angle measurement uncertainty at 15° mechanical mirror angle, showing capability of the accurate and precise characterization of multiple resonant MEMS mirrors.

REFERENCES

Brunner, D., Yoo, H.W., Thurner, T., and Schitter, G. (2019). Data based modelling and identification of nonlinear SDOF MOEMS mirror. In *Proc. SPIE 10931*, 1093117.

Druml, N., Maksymova, I., Thurner, T., van Lierop, D., Hennecke, M., and Foroutan, A. (2018). 1D MEMS Micro-Scanning LiDAR. In *Int. Conf. on Sensor Device Technologies and Appl.*

Isikman, S.O., Ergeneman, O., Yalcinkaya, A.D., and Urey, H. (2007). Modeling and Characterization of Soft Magnetic Film Actuated 2-D Scanners. *IEEE J. Sel. Topics Quantum Electron.*, 13(2), 283–289.

Ito, K., Niclass, C., Aoyagi, I., Matsubara, H., Soga, M., Kato, S., Maeda, M., and Kagami, M. (2013). System Design and Performance Characterization of a MEMS-Based Laser Scanning Time-of-Flight Sensor Based on a 256×64-pixel Single-Photon Imager. *IEEE Photon. J.*, 5(2), 6800114.

Kim, J.H., Jeong, H., Lee, S.K., Ji, C.H., and Park, J.H. (2017). Electromagnetically actuated biaxial scanning micromirror fabricated with silicon on glass wafer. *Microsyst. Technol.*, 23, 2075–2085.

Koh, K.H. and Lee, C. (2012). A Two-Dimensional MEMS Scanning Mirror Using Hybrid Actuation Mechanisms With Low Operation Voltage. *"J. Microelectromech. Syst.*, 21(5), 1124–1135.

Patterson, P.R., Hah, D., Fujino, M., Piyawattanametha, W., and Wu, M.C. (2004). Scanning micromirrors: an overview. In *Optomechatronic Micro/Nano Compon., Devices, and Syst.*, volume 5604, 195–208.

Rembe, C., Kant, R., and Muller, R.S. (2001). Optical measurement methods to study dynamic behavior in MEMS. In C. Gorecki, W.P.O. Jueptner, and M. Kujawinska (eds.), *Proc. SPIE. 4400*, 127–137.

Yalcinkaya, A.D., Urey, H., Brown, D., Montague, T., and Sprague, R. (2006). Two-axis electromagnetic microscanner for high resolution displays. *J. Microelectromech. Syst.*, 15(4), 786–794.

Yoo, H.W., Druml, N., Brunner, D.and Schwarzl, C., Thurner, T., Hennecke, M., and Schitter, G. (2018). MEMS-based lidar for autonomous driving. *Elektrotechnik und Informationstechnik*, 135(6), 408–418.

Yoo, H.W., Brunner, D., Thurner, T., and Schitter, G. (2019). Compensation for temperature dependency of 1D position sensitive detector. In *Proc. SPIE 10942*, 1094219.

Post-print version of the article: H. W. Yoo, D. Brunner, T. Thurner, G. Schitter, "MEMS Test Bench and its Uncertainty Analysis for Evaluation of MEMS Mirrors," *8th IFAC Symposium on Mechatronic Systems*, vol. 52, no. 15, pp 49-54, 2019. DOI: 10.1016/j.ifacol.2019.11.648